ISCI, Volume *21*

Supplemental Information

Bundled Three-Dimensional Human Axon Tracts Derived from Brain Organoids

D. Kacy Cullen, Wisberty J. Gordián-Vélez, Laura A. Struzyna, Dennis Jgamadze, James Lim, Kathryn L. Wofford, Kevin D. Browne, and H. Isaac Chen

Supplementary Information

Figures S1-S4

Transparent Methods

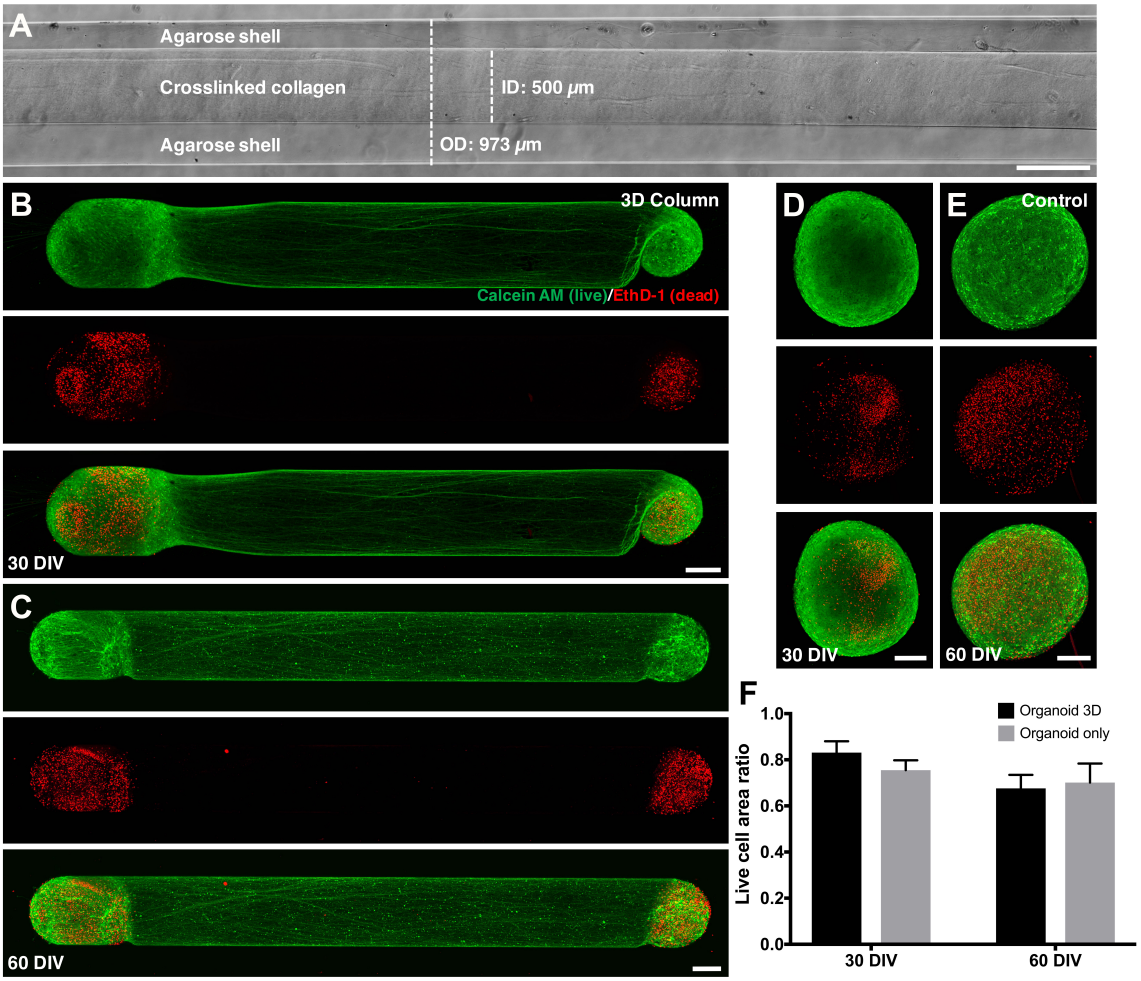

Figure S1. Assessment of cellular viability in organoid µTENNs (related to Figure 1). (A) Phase-contrast image of a micro-column prior to organoid insertion with an outer diameter (OD) and inner diameter (ID) of 973 µm and 500 µm, respectively. The image shows the agarose shell surrounding the inner core composed of crosslinked collagen. Representative confocal reconstructions of bidirectional iPSC-derived organoid µTENNs grown in 0.5-cm micro-columns for 30 (B) and 60 DIV (C) stained for live (calcein AM; green) and dead cells (EthD-1; red). Time-matched organoids floating in media served as controls (D: 30 DIV, E: 60 DIV). (F) There were no significant differences in the live cell

area ratio between 3D and planar cultures over time. Data presented as mean ± SEM. Scale bars: 500 μm (A), 200 μm (B-E).

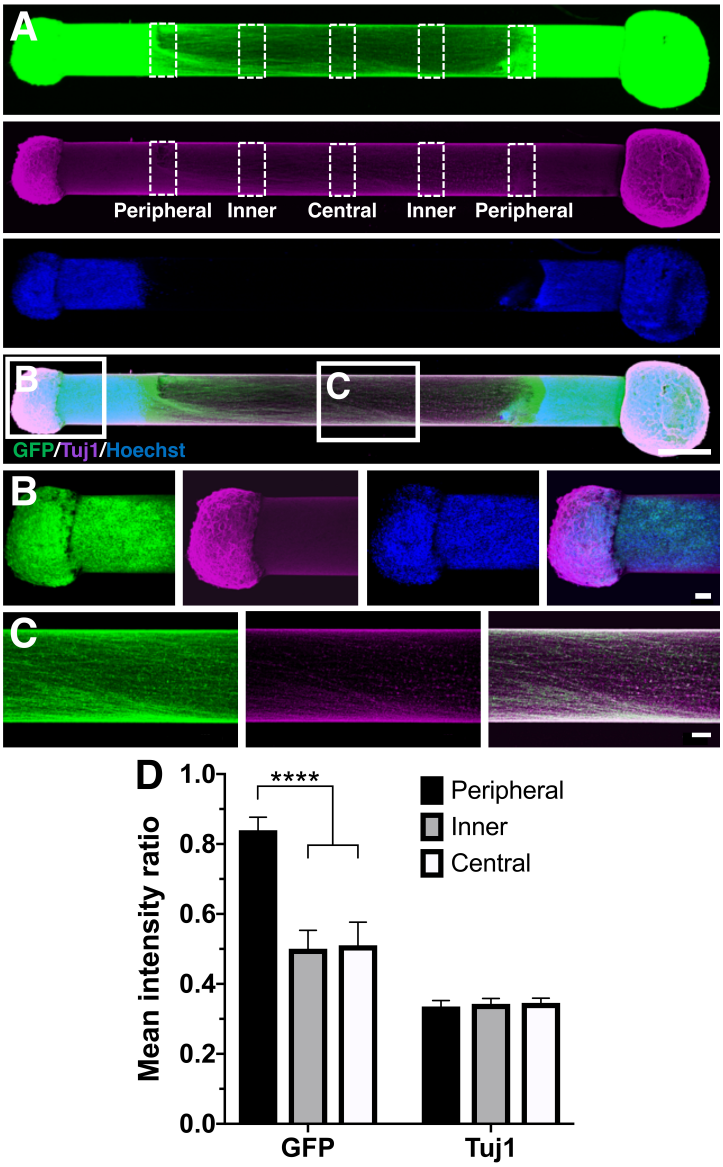

Figure S2. Immunocytochemical analysis of 0.5-cm bidirectional ESC-derived µTENNs (related to Figure 2). (A) Confocal reconstruction of a representative 0.5-cm GFP+ ESC-derived organoid µTENN at 24 DIV stained for Tuj1 (magenta) and Hoechst (blue). There was a distinct separation between regions containing neural somata and neurites. By 24 DIV, neurites had projected across the entire length of the micro-column. Box insets in the merged image of A correspond to higher magnification images of the

organoid cell aggregate (B) and neurites in the central region of the μTENN (C). (D) Neurite outgrowth was quantified as the mean GFP and Tuj1 intensity in five regions of interest (see A) normalized relative to the maximum intensity in the organoid cell mass. Intensity values were statistically similar in the inner and central regions at 24 DIV, demonstrating robust neurite extension across the entire micro-column. Data presented as mean ± SEM (**** $p < 0.0001$; Tukey's multiple comparisons test). Scale bars: 500 μm (A), 100 μm (B-C).

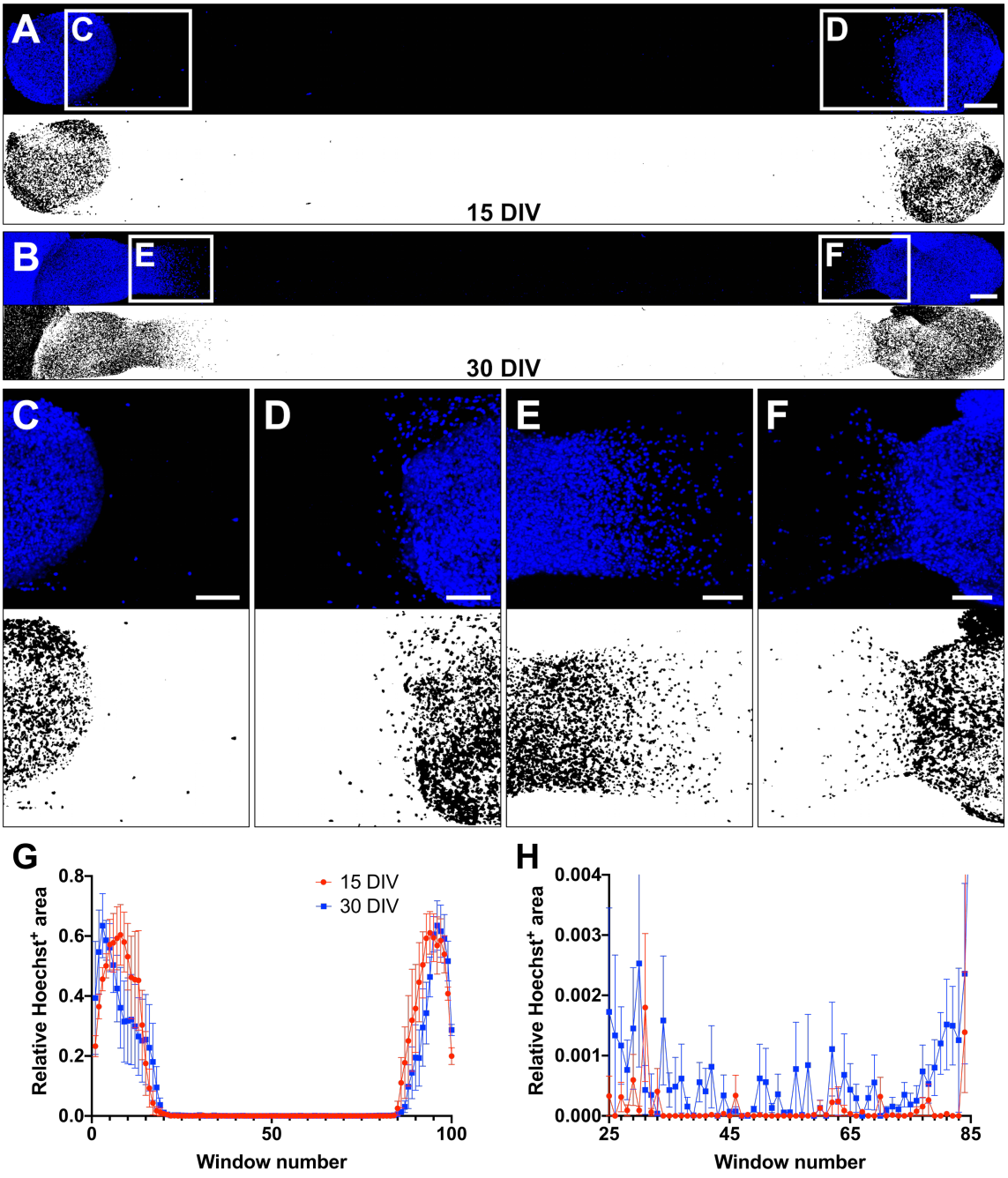

Figure S3. Analysis of cell migration from the organoid mass within micro-columns (related to Figure 3). Bidirectional iPSC-derived organoid µTENNs were cultured for 15 (A) and 30 DIV (B) within 0.5-cm micro-columns, fixed, and stained for nuclei (Hoechst; blue). The binary images of the Hoechst channel are also shown. Higher

magnification images display areas close to the organoid edge in A (C-D) and B (E-F), showing qualitatively a greater degree of local migration at 30 DIV. (G) Cell migration was assessed by measuring the black particle areas (Hoechst+ regions) in the binary images in 100 windows along the length of the construct. The Hoechst+ area was normalized to window size and presented here as a function of window number, where 1 and 100 correspond to the far-left and far-right edges of the Hoechst channel image, respectively. (H) Zoom-in of the graph in G in the region between windows 25 and 85, corresponding to the more central regions of the μTENNs. Data presented as mean ± SEM. Scale bars: 150 μm (A), 200 μm (B), 100 μm (C-F).

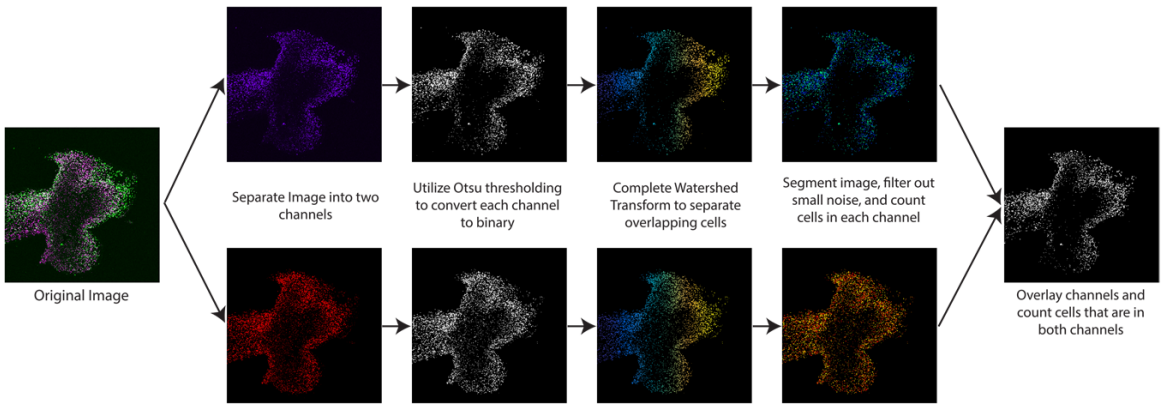

Figure S4. Workflow of automated cell counting (related to Figure 3). Separate color channels were converted to a binary image. A watershed transform was then performed to separate overlapping cells. The resulting image was segmented and filtered to remove noise, and cell counting was performed on this processed image. Combining the processed images for both color channels allowed for counting of the co-labeled cells.

Transparent Methods

Pluripotent stem cell maintenance

The H9 human embryonic stem cell (ESC) line (NIH code WA09; Wicell, Madison, WI) expressing enhanced green fluorescent protein (GFP) driven by the chicken actin promoter (H9-GFP; Children's Hospital of Philadelphia Stem Cell Core, Philadelphia, PA) was generated using zinc finger nucleases to target the expression construct to the AAVS1 locus (Paluru et al., 2014). The C1.2-GFP and C1.2-red fluorescent protein (RFP) lines were created via lentiviral transduction of the C1.2 induced pluripotent stem cell (iPSC) line (BJ-ATCC CRL-2522). All cell lines were maintained on mouse embryonic fibroblast (MEF) feeder cells (CF-1; MTI-Globalstem, Gaithersburg, MD). MEFs were plated one day before passaging at a density of $2x10^5$ cells per well in a 0.1% gelatin-coated 6-well plate (Millipore Sigma, Burlington, MA). Stem cells were cultured in human embryonic stem cell (hES) media containing the following components: DMEM/F12 (Invitrogen, Carlsbad, CA), 20% KnockOut serum replacement (Invitrogen), 1 mM non-essential amino acids (Invitrogen), 1X GlutaMax (Invitrogen), 0.1 mM β-mercaptoethanol (Sigma-Aldrich, St. Louis, MO), 100 U/mL penicillin/100 μg/mL streptomycin (Invitrogen), and 6 ng/mL bFGF (R&D Systems, Minneapolis, MN). Colonies were passaged with TryPLE (Thermo-Fisher, Waltham, MA) or collagenase type IV (Invitrogen) every 7 days. Passage numbers were between 110-135 (H9-GFP) or 20-45 (iPS lines). All cell lines were confirmed to be negative for mycoplasma contamination. Early passage stocks of the cell lines were karyotyped to confirm their genomic integrity (Cell Line Genetics, Madison, WI).

Generation of brain organoids

Brain organoids were generated using a protocol modified from Pasca, et al., 2015. In brief, stem cell colonies were grown until they were approximately 3-4 mm in diameter, after which they were detached by incubation with collagenase type IV for 45-60 minutes at 37^{o}C. The detached colonies were washed once with hES media and then placed in ultra-low attachment 6-well plates (Corning, Corning, NY) in Induction Media consisting of hES media supplemented with 100 nM LDN193189 (Stemgent, Cambridge, MA), 10 µM SB431542 (Stemgent), 2 µM XAV939 (Stemgent), and 10 µM Y-27632 (Tocris Biosciences, Bristol, United Kingdom). From differentiation day (dd) 1-6, the developing embryoid bodies were maintained in Induction Media without Y-27632 with daily media changes. From dd6 onwards, embryoid bodies were cultured on an orbital shaker. From dd6-25, the developing organoids were maintained in Neuronal Media consisting of Neurobasal media (Invitrogen) supplemented with 1:50 B27 without vitamin A (Invitrogen), 1X Glutamax (Invitrogen), 100 U/mL penicillin/100 µg/mL streptomycin (Invitrogen), 20 ng/mL bFGF (R&D Systems), and 20 ng/mL EGF (R&D Systems) with daily media changes until dd17 and then every other day afterwards. From dd25-43, every other day media changes with Neuronal Media supplemented with 20 ng/mL NT3 (R&D Systems) and 20 ng/ML BDNF (R&D Systems) were performed. After dd43, every other day media changes with Neuronal Media without growth factors were performed. Developing iPSC-derived organoids were cut at dd30-35 with sterile fine-tip forceps to a diameter less than 500 µm. Organoids derived from ESC and iPSC cells used for µTENN construction were between dd100-150 and dd62-79, respectively.

Fabrication of micro-column constructs

All materials were obtained from Invitrogen, BD Biosciences, or Sigma-Aldrich unless otherwise noted. The outer hydrogel shell of the micro-columns, which consisted of 1% agarose in Dulbecco's phosphate-buffered saline (DPBS) and had an outer diameter of 973 μm, was generated by drawing the agarose solution into a capillary tube (Drummond Scientific, Broomall, PA) via capillary action. An acupuncture needle (500 μm diameter; Seirin, Weymouth, MA) was inserted into the center of the agarose-filled capillary tube before agarose polymerization to produce space for an inner core. As the micro-columns gelled, a collagen solution was prepared on ice, consisting of 1 mg/mL rat tail type I collagen and the cross-linking agents 11.70 mM N-(3-Dimethylaminopropyl)-N'-ethylcarboimide hydrochloride, 4.3 mM N-Hydroxysuccinimide, and 35.6 mM sodium phosphate monobasic. Afterwards, the needle was removed, and the collagen solution was suctioned into the lumen formed by the needle to fill it completely. The micro-columns with collagen were then incubated at 37ºC for 30 min to allow the collagen to polymerize and cross-link. Finally, the micro-columns were pushed out of the capillary tubes using a 20-gauge needle into DPBS, sterilized under UV light for 30 min, and stored overnight at 37 ºC. The micro-columns then were rinsed twice with warm DPBS to remove remaining traces of the cross-linking agents, transferred to dishes with warm culture media, and then cut to the desired length (1-10 mm).

Organoids derived from ESC cells were cut into small pieces using fine-tip forceps and immediately inserted into one or both ends of the micro-columns under a dissection scope. In some cases, the organoids were subsequently trimmed with forceps to fit fully within the micro-column. Only iPSC-derived organoids that precisely fit

within the micro-column lumen without additional cutting were used in fabricating this type of μTENN. For planar cultures, organoids were plated on tissue culture plates pre-treated with 20 μg/mL poly-d-lysine at room temperature overnight followed by 20 μg/mL laminin at room temperature for 2 hours.

Immunohistochemical analysis of organoid μTENNs

Whole constructs were fixed in 4% formaldehyde for 35 min and permeabilized using 0.3% Triton X-100 (Sigma-Aldrich) plus 4% horse serum (HS; Invitrogen) for 60 min at room temperature. Primary antibodies (see below) diluted in phosphate-buffered saline (PBS, Sigma-Aldrich)/4% HS were applied overnight at 4°C. Appropriate fluorescent secondary antibodies (Alexa-488, -594 and/or -649 [Invitrogen] diluted 1:500 in PBS/4% HS/30 nM Hoechst [Invitrogen]) were applied for 2 hours at room temperature.

Organoid μTENNs were also analyzed using paraffin-embedded sections. Whole constructs were fixed in 4% formaldehyde for 35 min and processed through a 6-hour cycle of ascending concentrations of ethanol and xylene. The constructs were then embedded in paraffin, sectioned at 12 μm, and mounted on Superfrost Plus slides (Thermo-Fisher). Sections were dewaxed through 2 changes of xylene and rehydrated through 2 changes of 100% ethanol, 2 changes of 95% ethanol, and distilled water. For identification of neurons (Tuj-1, MAP2), astrocytes (GFAP), and neural progenitors (Pax6), sections were subjected to modified pressure-cooker/microwave antigen retrieval using TRIS-EDTA buffer for 8 min. Following antigen retrieval, sections were blocked for 30 minutes using blocking serum from the Vectastain Elite Universal Kit (Vector

Labs, PK-6200) in Optimax Wash Buffer (Biogenex, HK583-5K). For identification of layer-specific markers (CTIP2, Satb2), sections were dewaxed and rehydrated as above. They were then subjected to antigen retrieval using 10 mM sodium citrate buffer (pH 6.0) for 30 min at 100 ºC. Sections were cooled and blocked with 5% HS in Optimax Wash Buffer for 30 minutes. Primary antibodies diluted in PBS/4% HS (see below) were applied overnight at 4 ºC. The slides were then washed 3 x 5 minutes in PBS/TWEEN (Sigma), and secondary antibodies (1:500 in PBS/4% HS/30 nM Hoechst) were applied for 1 hour at room temperature. Slides were washed 3 x 5 min with PBS/TWEEN prior to coverslipping with Fluoromount G.

Primary antibodies include Tuj-1 (Sigma T8578, mouse, 1:750), tau (Dako A0024, rabbit, 1:500), MAP2 (Abcam 53992, chicken, 1:1000), MAP2 (Abcam ab11267, mouse, 1:1000), GFAP (Millipore MAB5804, rabbit, 1:500), synapsin I (Synaptic Systems 106-001, mouse, 1:1000), Satb2 (Abcam ab51502, mouse, 1:100), CTIP2 (Abcam ab18465, rat, 1:200), Pax6 (Biolegend 901301, rabbit, 1:100), human nuclear antigen (Millipore MAB1281, mouse, 1:1000).

Imaging

Whole, non-sectioned constructs were imaged with phase-contrast and epifluorescence microscopy using a Nikon Eclipse Ti-S microscope. Images were acquired using an QiClick camera interfaced with NiS Elements software (Nikon). Confocal microscopy was performed on non-sectioned and sectioned constructs using an A1RSI laser scanning confocal microscope (Nikon). Confocal images were reconstructed from full thickness z-stacks. To obtain transverse cross-sections of the axonal tract region

in immunostained μTENNs, constructs were placed vertically in a block of 5% agarose with a preformed orifice that fit the micro-column. The construct was then imaged using a 16x immersion objective and a Nikon A1RMP+ multi-photon microscope linked with NiS Elements AR 4.60.00.

Neurite outgrowth quantification

The length of neurite outgrowth in organoid μTENNs was determined by measuring the distance from the organoid cell mass to the longest observable neurite using Fiji (NIH) in confocal images taken from live constructs at 1, 4, 7, 10, 30, 40, and 50 DIV (n = 4 for all time points except for n = 6 at 30, 40, 50 DIV). GFP+ organoids from the same differentiation batch also were cultured on laminin-coated planar surfaces as controls. In this case, the length of growth was quantified by tracing the length of the longest neurite from phase contrast images taken at 1, 4, 7, 10, and 30 DIV using the Simple Neurite Tracer plugin (n = 9 at all time points except n = 3 at 30 DIV because of organoid detachment). Imaging and quantification of controls stopped after 30 DIV because all organoids had detached. The length change rate at each time point was estimated based on the previous time point by the backward difference method. Differences in outgrowth and growth rate between time points in 3D micro-columns and between planar controls and 3D micro-columns were assessed with one-way analysis of variance (ANOVA) and two-way ANOVA, respectively, with Tukey's test for multiple comparisons ($p < 0.05$ as the criterion for statistical significance). These analyses, and all below unless otherwise noted, were carried out in Prism 8 (GraphPad).

Neurite density quantification

To compare the neurite density along micro-columns, five regions of interest (ROI) of equal size (163 pixels x 80 pixels) were selected in the GFP and Tuj1 channels along the region spanned by axon tracts (n = 3 constructs for each group) in ESC-derived organoid µTENNs. Two peripheral ROIs were chosen adjacent to the organoid cell mass, two inner ROIs were selected with their center at 25 and 75% of the length of the neurite region, and one central ROI was located midway along the neurite region. The ROIs were cropped and converted to 8-bit images using ImageJ (NIH), and the mean gray scale value was measured. These values were corrected for background fluorescence by subtracting the mean gray scale values derived from three randomly selected background regions (163 pixels x 80 pixels) in the original images. To facilitate comparisons across samples, these background-corrected values were normalized relative to the maximum gray scale value in the organoid cell mass region of each sample. Normalized values were averaged across each ROI group (n = 6 for peripheral and inner and n = 3 for central ROIs). Pairwise differences were evaluated with Tukey's test for multiple comparisons ($p < 0.05$ as the threshold for statistical significance).

Assessment of organoid cell mass size

ImageJ was used to measure the area of the organoid cell mass in the Hoechst channel in whole hESC-derived organoid µTENNs. These values were averaged across samples from each group. An unpaired t-test was applied to compare the somatic size between conditions ($p < 0.05$ as the threshold for statistical significance).

Automated Satb2+ and CTIP2+ cell counting

Counting of Satb2+ and CTIP2+ cells in ESC-derived organoid µTENN sections was performed utilizing a custom MATLAB script. This automated, feature-based segmentation methodology was comprised of the following sequential steps (Figure S4). Color images (Satb2 or CTIP2) were converted to a greyscale binary image using Otsu's thresholding. In regions of high cell density, the binary mask represented overlapping cells as connected components, which would result in undercounting of cells. In order to correct for overlapping cells, the binary images were pre-processed with a distance transform gradient, and a watershed transform was then applied to separate clustered cells. Following the watershed transform, individual cells were segmented and counted to generate the number of Satb2+ and CTIP2+ cells. To count the number of Satb2+/CTIP2+ cells, segmented Satb2 and CTIP2 images were overlaid on top of each other. Object coordinates that were positive for both signals were preserved while image coordinates with one or no signals were eliminated. The remaining segmented components represented cells that were double-positive and were quantified. The number of double-positive cells was subtracted from the Satb2 and CTIP2 cell counts to compute the number of Satb2-only and CTIP2-only cells, respectively.

Characterization of organoid tissue structure

The degree of organoid tissue structure in ES-derived organoid µTENN sections was scored using a 0-2 scale (0=no organization, 1=geographic segregation of Satb2+ and CTIP2+ cells but no laminar structure, 2=laminar structure) by three authors (DKC, WG, HIC) who were blinded to the other authors' scores. Mean organization scores were then

calculated. These scores were used to compare sides within organoid μTENN constructs over time. Organization scores were compared across time points with an unpaired *t* test. Data segregated by organization classification and time points were analyzed with a two-way ANOVA. Frequency of cellular phenotypes was compared across phenotype and time points using two-way ANOVAs. If differences were detected between groups, Tukey's post hoc test was employed with a Bonferroni correction to account for multiple comparisons ($p < 0.05$ was considered significant). All analyses were carried out in R Studio Version 1.0.143.

Analysis of neuronal migration

The extent of neuronal migration from the organoid mass within μTENNs was evaluated using bidirectional iPSC-derived brain organoid μTENNs cultured for 15 and 30 DIV ($n = 4$ each) within 0.5-cm micro-columns. After incubation of fixed constructs for 10 min with Hoechst (1/10,000 in PBS), these μTENNs were imaged, and the Hoechst channel was analyzed for cell migration. First, binary masks of the images were made in Fiji and precisely cropped to encompass only the width of the lumen and the distance from organoid to organoid. The Hoechst+ area was measured in 100 windows of equal width along this distance and normalized relative to the window area using a custom-made MATLAB script. Differences between normalized Hoechst+ areas as a function of window number and time were assessed with two-way ANOVA and Sidak's multiple comparisons test ($p < 0.05$ was significant).

Viability quantification

We assessed viability in hiPSC-derived organoids at 30 and 60 DIV using bidirectional μTENNs (n = 6 constructs at each time point) and controls consisting of organoids cultured floating in media (n = 7 at each time point). Organoid μTENNs and controls were rinsed once in DPBS and incubated in 1/2000 calcein-AM and 1/500 ethidium homodimer-1 (EthD-1) (ThermoFisher) in DPBS for 30 min at 37ºC. After two rinses in DPBS, whole constructs and controls were imaged using confocal microscopy, and the maximum intensity projection of the z-stacks was taken. To estimate viability within the organoid mass, the green (calcein-AM+) and red (EthD-1+) channels of the projection were converted to 8-bit images using Fiji. Subsequently, the images were binarized by setting manual global thresholds to obtain cell-shaped regions; different thresholds were chosen for each image given that consistent values did not accurately reflect intrinsic differences in each image. The areas of calcein AM+ and EthD-1+ cells were quantified only in the organoid mass region, and the live cell area ratio was defined as the ratio of calcein AM+ area over the total area of calcein AM+ and EthD-1+ cells. Differences in viability in terms of time and group were analyzed using two-way ANOVA with Tukey's test for multiple comparisons ($p < 0.05$ was considered significant).

Analysis of organoid integration and calcium signaling

Bidirectional μTENNs were fabricated with a GFP+ and RFP+ organoid on either end of a 1-mm micro-column. These constructs were imaged with confocal microscopy at different time points, and the distances between the longest GFP+ and RFP+ neurite and the edge of the GFP+ and RFP+ organoid were measured. To approximate the time for

differential neurite crossing and integration with the other organoid mass, the normalized neurite position was defined as the organoid-specific (GFP+ or RFP+) neurite length relative to the distance between the two organoids. With this definition, 0 and 1 referred to the edges of the GFP+ and RFP+ organoid, respectively.

Calcium activity was assessed after culturing iPSC-derived, non-fluorescent, bidirectional organoid μTENNs for 15 DIV (dd77 at imaging) in a 1-mm micro-column. The constructs were incubated with 5 μM Fluo-4 (Thermo Fisher Scientific) in Neuronal Media without growth factors for 30 min at 37°C and then rinsed with media before imaging. Calcium imaging was performed in Neuronal Media at room temperature using a 10x objective and Nikon A1RMP+ multi-photon microscope paired with NiS Elements AR 4.60.00. Videos were recorded at 5 frames per second.

Selection of ROIs and extraction of mean gray values were performed using ImageJ. Calcium responses were calculated using Fluoro-SNNAP software. In brief, background was subtracted from the signals in each sample, and then, $\Delta F/F0$ values were calculated for each ROI using the 10th percentile value of the complete raw fluorescence trace as *F0*. Identification of calcium events and calculation of synchronization indices (scale of 0–1) within and between organoids were also done with FluoroSNNAP. For each sample, 6 ROIs around active neuronal somata were selected for these analyses. Default FluoroSNNAP settings, including the reference calcium waveform library, were used.